

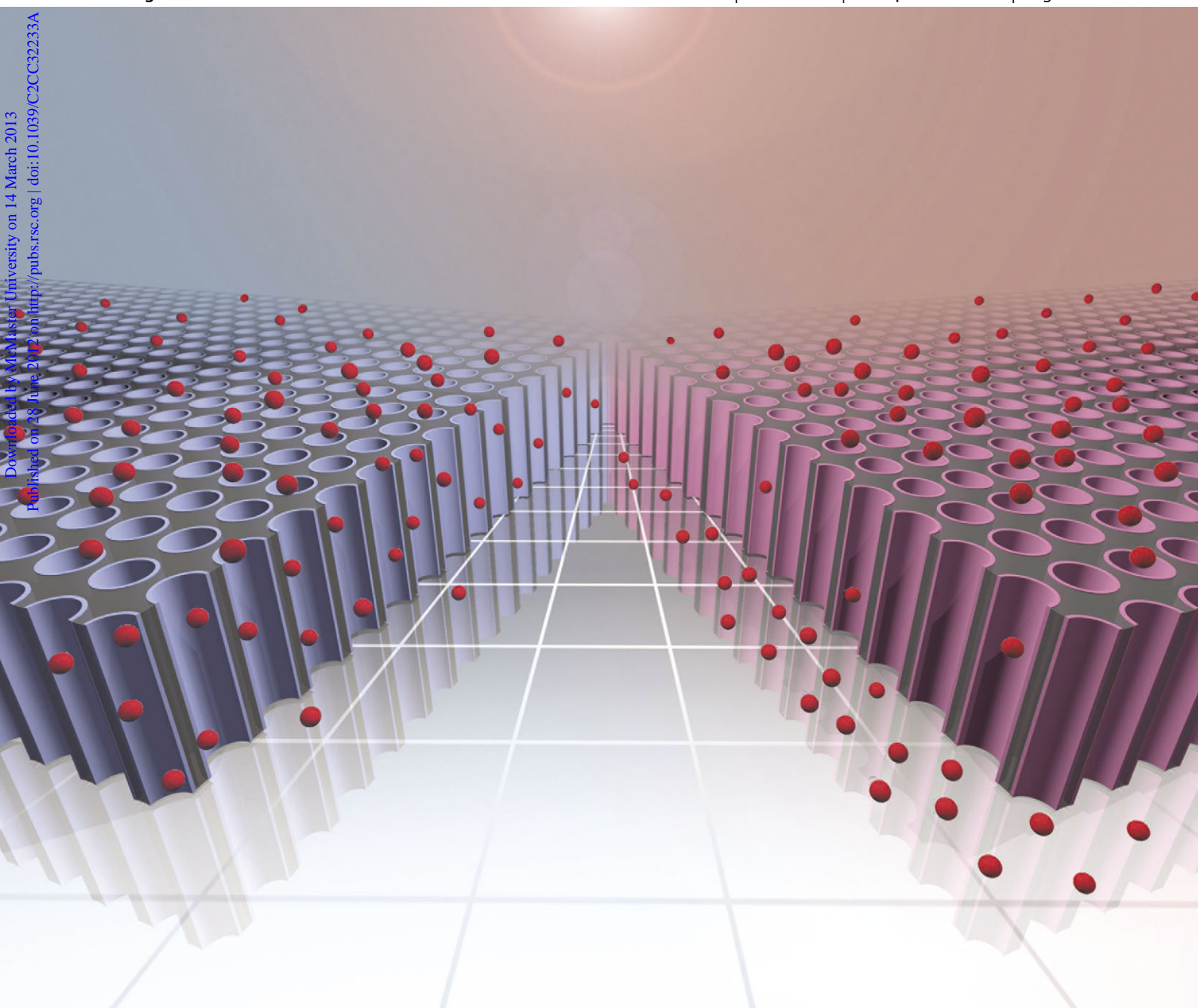
# ChemComm

Chemical Communications

www.rsc.org/chemcomm

Volume 48 | Number 74 | 25 September 2012 | Pages 9197–9320

Downloaded by Maastricht University on 14 March 2013  
Published on 28 June 2012 on http://pubs.rsc.org | doi:10.1039/C2CC32233A



ISSN 1359-7345

RSC Publishing

**COMMUNICATION**

Jee Seon Kim, Yoon Sung Nam *et al.*  
Thermally controlled wettability of a nanoporous membrane grafted with catechol-tethered poly(*N*-isopropylacrylamide)



1359-7345(2012)48:74;1-W

Cite this: *Chem. Commun.*, 2012, **48**, 9227–9229

www.rsc.org/chemcomm

## COMMUNICATION

Thermally controlled wettability of a nanoporous membrane grafted with catechol-tethered poly(*N*-isopropylacrylamide)<sup>†</sup>Jee Seon Kim,<sup>\*a</sup> Taek Gyung Kim,<sup>b</sup> Won Ho Kong,<sup>a</sup> Tae Gwan Park<sup>a</sup> and Yoon Sung Nam<sup>\*acd</sup>

Received 27th March 2012, Accepted 27th June 2012

DOI: 10.1039/c2cc32233a

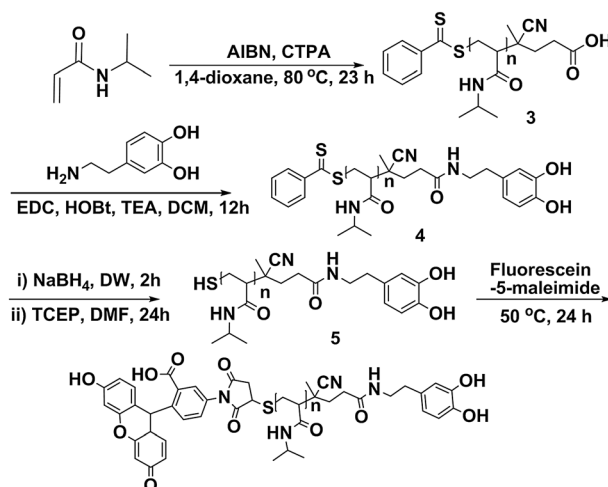
A nanoporous membrane is coated with catechol-tethered poly(*N*-isopropylacrylamide). The thermosensitive variation of surface wettability determines the hindered diffusivity of dextran (40 kDa) through the nanopores.

Surface modification of nanoporous inorganic materials with functional polymers has received increasing attention because of a wide range of applications, including nanofluidics, drug delivery, separation, and biosensors.<sup>1</sup> Two approaches are available for the polymer coatings of nanoporous structures: direct coatings of pre-synthesized polymers and reactive polymer coatings. Spin or dip coatings of pre-synthesized polymers often lead to nanoscale heterogeneity in surface topography. Reactive polymer coatings, based on the surface deposition of initiators followed by surface polymerization, have been also used to modify the surface of a variety of substrates. To avoid the polymer blocking of nanopores, the pre-activation of surfaces is essential for the surface-selective grafting of polymer chains.<sup>2</sup>

Recently, a mussel-inspired polymer coating was investigated as a simple and versatile method for a variety of substrates.<sup>3</sup> To this end, catechol and its derivatives have been used as biomimetic adhesion molecules. They are known to have a strong binding affinity to metal oxide through the metal–catechol coordination, which is robust enough to resist thermal and hydrolytic decomposition in an aqueous milieu.<sup>4</sup> In addition, catechol has been employed as a pendant or end group of a pre-synthesized polymer for functional polymer coatings of various substrates.<sup>5</sup>

This study introduces a simple one-step coating method to modify the surface of nanoporous materials using a

catechol-functionalized polymer. An anodized aluminium oxide (AAO) membrane was chosen as a substrate because of the well-defined nanopore structure. Monodisperse poly(*N*-isopropylacrylamide) (PNIPAAm) was synthesized by reversible addition fragmentation chain transfer (RAFT) polymerization. PNIPAAm has been extensively studied as a thermally-responsive polymer as it exhibits a sharp coil-to-globule transition at a lower critical solution temperature (LCST) of ~32 °C in aqueous solution.<sup>6</sup> 4-Cyano-4-((thiobenzoyl)sulfanyl)pentanoic acid (CTPA) was synthesized and used as a RAFT agent to prepare bi-functional PNIPAAm having carboxylic acid and dithioester at each end (Scheme 1 and ESI<sup>†</sup>). The measured molecular weight of the synthesized PNIPAAm was 12 kDa with a polydispersity index of 1.09. To graft PNIPAAm to the surface of nanopores, catechol was conjugated as a binding moiety to the terminal carboxylic acid of the synthesized PNIPAAm *via* a simple amide coupling reaction. Catechol-conjugated PNIPAAm (denoted 'PNIPAAm-ct') was produced with a yield of 94%. To modify the surface of alumina nanopores with a nominal diameter of 20 nm, 1 wt% aqueous solution of PNIPAAm-ct was infiltrated through an AAO membrane (see ESI<sup>†</sup> for more details). Compared to dip coating, filtration is advantageous for the homogeneous deposition of polymers on the surface of nanopores because convective flow



Scheme 1 Synthetic scheme of catechol-conjugated PNIPAAm.

<sup>a</sup> Department of Biological Sciences, Korea Advanced Institute of Science and Technology, Daejeon 305-701, Republic of Korea. E-mail: eliekim@kaist.ac.kr

<sup>b</sup> Severance Hospital Integrative Research Institute for Cerebral & Cardiovascular Diseases, Yonsei University Health System, Seoul, 120-752, Republic of Korea

<sup>c</sup> Department of Materials Science and Engineering, Korea Advanced Institute of Science and Technology, Daejeon 305-701, Republic of Korea

<sup>d</sup> KAIST Institute for NanoCentury (KINC) and BioCentury (KIB), Korea Advanced Institute of Science and Technology, Daejeon 305-701, Republic of Korea. E-mail: yoonsung@kaist.ac.kr; Fax: +82 42 350 3310; Tel: +82 42 350 3311

<sup>†</sup> Electronic supplementary information (ESI) available: Detailed experimental procedures, NMR data, and equations for diffusivity and grafting density. See DOI: 10.1039/c2cc32233a

keeps removing unbound and weakly-bound polymers from the pore surface, minimizing non-specific binding and pore blocking.

FT-IR and XPS analyses indicated the successful surface modification of an AAO membrane with PNIPAAm-ct. The FT-IR spectrum of a bare membrane showed only broad absorption bands of Al–O stretching at  $490\text{ cm}^{-1}$  and  $580\text{ cm}^{-1}$ , while the PNIPAAm-grafted membrane exhibited several characteristic absorption peaks for catechol and PNIPAAm: hydrogen-bonded catechol (O–H stretching) at  $3280\text{ cm}^{-1}$ , aromatic (C–H stretching) at  $3075\text{ cm}^{-1}$ , methylene (C–H stretching) at  $2889\text{ cm}^{-1}$ , carbonyl (C=O stretching) at  $1600\text{ cm}^{-1}$ , and isopropyl (C–H stretching) at  $1360\text{ cm}^{-1}$  (Fig. 1a). XPS analysis was also carried out to confirm the immobilization of PNIPAAm onto the alumina membrane. The bare membrane had only Al and O1s peaks with peak area percentages of 37.7% and 46.8%, respectively. The C1s signal of the bare membrane was ascribed to foreign organic contaminants. The PNIPAAm-grafted membrane, on the other hand, showed the appearance of the N1s signal and the increased C1s signal to 28.3%, confirming the immobilization of PNIPAAm (Fig. 1b and Table S1 in ESI†).

To fluorescently tag PNIPAAm-ct, the dithioester end group of PNIPAAm-ct was reduced to a free thiol end group by sodium borohydride. PNIPAAm-ct (**4**) was converted to a mixture of thiol-PNIPAAm-ct and its dimers linked by a disulfide bond (see Scheme 1b). The disulfide-bonded dimer showed a higher molecular weight, as shown in Fig. 1c. Tris-(2-carboxyethyl)phosphine hydrochloride (TCEP) was used as a reducing agent to dissociate the dimer of thiolated compounds, finally exposing a free thiol group at the end of PNIPAAm (**5**) for the conjugation to fluorescein-5-maleimide.<sup>7</sup> The confocal fluorescence images of the membrane treated with the fluorescein-labeled PNIPAAm (**6**) showed that PNIPAAm-ct was homogeneously grafted to the internal surface of nanopores within the membrane (Fig. 2a and b). The AAO membrane treated with free fluorescein-5-maleimide did not show any significant fluorescence signals from

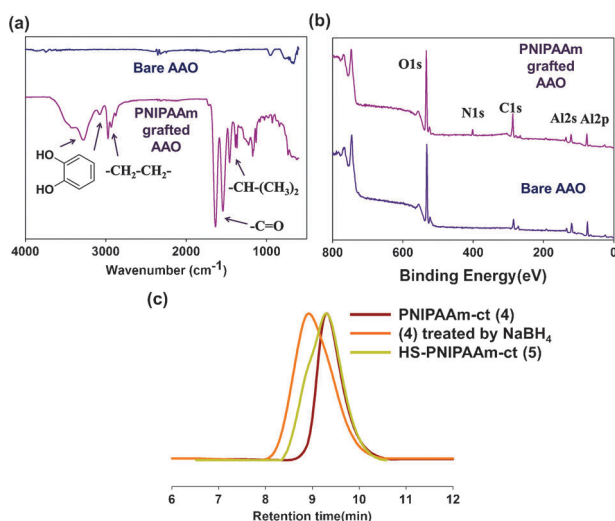


**Fig. 1** FT-IR (a) and XP (b) spectra of the PNIPAAm-grafted and bare membranes. The XP spectra were calibrated with the C1s emission peak for  $\text{sp}^3$ -hybridized carbons at 284.5 eV; (c) GPC diagrams of the synthesized PNIPAAm-ct (**4**) (red),  $\text{NaBH}_4$ -treated PNIPAAm-ct (orange), and HS-PNIPAAm-ct (**5**) (yellow).

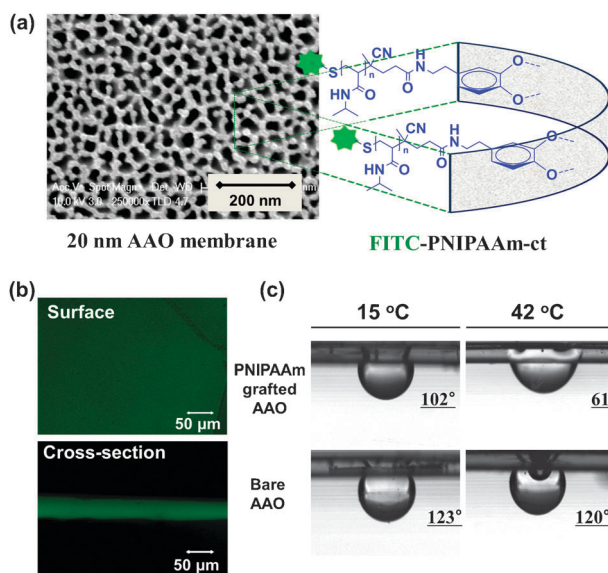


**Fig. 2** (a) Schematic illustration of the PNIPAAm grafted AAO membrane; (b) confocal fluorescence images of the AAO membrane treated with fluorescein-labeled PNIPAAm-ct: surface (upper panel) and cross-section (lower panel); (c) static oil-contact angle images of the bare and PNIPAAm-grafted AAO membranes at temperatures below and above the LCST.

the cross-section of the membrane (data not shown), indicating that the small fluorescent dye penetrated the pore without binding to the pore surfaces. This result suggests that the catechol moiety of the polymer is responsible for the successful grafting of PNIPAAm to the AAO nanopores.

The static oil-contact angle was measured to examine the temperature-responsive modulation of the surface wettability of the PNIPAAm-grafted AAO membrane (Fig. 2c). The surface of a bare AAO membrane was very hydrophilic – the static contact angle of silicone oil ( $\theta$ ) was *ca.*  $120^\circ$  (the water contact angle is known to be below  $10^\circ$ ) and almost independent of temperature change. By contrast, the contact angle of the PNIPAAm-grafted surface was highly affected by temperature variation presumably through the conformational changes of the grafted PNIPAAm chain. The PNIPAAm-grafted AAO membrane maintained the hydrophilic surface below the LCST ( $\theta = 102^\circ$  at  $15^\circ\text{C}$ ); however, at  $42^\circ\text{C}$  the contact angle dramatically decreased to  $\theta = 61^\circ$ , indicating the increased surface hydrophobicity induced by the shrinkage of the PNIPAAm chains.

We determined the thermally-induced changes of molecular diffusivity of a solute within the PNIPAAm-grafted nanopores. A fluorescein–dextran conjugate (FITC–dextran, 40 kDa) with an equivalent hydrodynamic diameter of 7.5 nm was chosen as a solute.<sup>8</sup> The effective diffusivity within the membrane was measured using a Franz-type diffusion cell at temperatures above and below the LCST. It was expected that the diffusion rate of FITC–dextran within the membrane would be responsive to temperature variation *via* the conformational change of the grafted PNIPAAm chain;<sup>9</sup> however, it was not simply predictable because hindered diffusion through a pore of comparable size can be affected by the hydrodynamic factor for the interaction between solutes and pore surface as well as the steric hindrance due to the pore blocking.



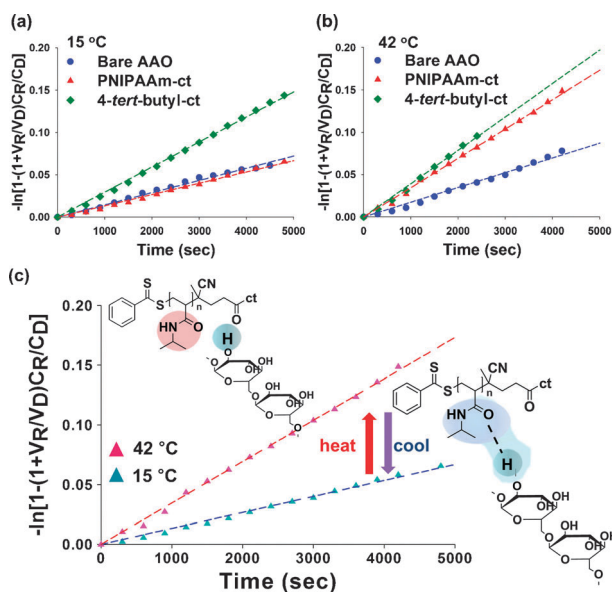


**Fig. 3** Permeability of unmodified (blue circle), PNIPAAm-grafted (red triangle) and 4-*tert*-butylcatechol (green diamond), 20 nm pore AAO membrane measured using FITC-dextran at temperatures below (a) and above (b) the LCST of PNIPAAm; (c) thermally responsive permeability of the PNIPAAm-grafted, 20 nm pore AAO membrane (eqn (S1) used for this plot is described in ESI†).

The measured diffusivities of FITC-dextran within the bare membrane were  $8.48 \times 10^{-9} \text{ cm}^2 \text{ s}^{-1}$  at 15 °C and  $1.02 \times 10^{-8} \text{ cm}^2 \text{ s}^{-1}$  at 42 °C. The slightly higher diffusivity at 42 °C seems to be caused by the increased thermal motion of FITC-dextran. Within the nanopores grafted with PNIPAAm-ct, the diffusivity at 15 °C was  $7.94 \times 10^{-9} \text{ cm}^2 \text{ s}^{-1}$ , which is similar to the value of the bare membrane though the actual pore size of the PNIPAAm-grafted membrane was reduced to 64% of the size of the bare pore. The diffusivity of FITC-dextran through the nanopores was calculated using a ‘hindered diffusion’ model equation to clarify the contribution of the partial unblocking to the increased diffusivity. The effective diffusion coefficient is determined by both the steric restriction resulted from the pore blocking and the interaction between the surface of the pore wall and solutes, as described in ESI† in more detail. The calculated diffusivity in the polymer-grafted pores at 15 °C was  $6.11 \times 10^{-9} \text{ cm}^2 \text{ s}^{-1}$ , which was only 77.0% of the experimental value, indicating that the hydrodynamic effect is more significant than pore blocking in the hindered diffusion through the PNIPAAm-grafted nanopores. Very interestingly, the diffusivity of FITC-dextran at 42 °C greatly increased to  $2.03 \times 10^{-8} \text{ cm}^2 \text{ s}^{-1}$ , which is 2.5 times larger than that at 15 °C (Fig. 3). The dramatically increased diffusivity at 42 °C is not only attributed to the reduced size or blocking of nanopores, which is the reason widely adopted in the similar systems.<sup>2,9</sup> In our system, the extended length of PNIPAAm used in this study was much smaller than the size of nanopores. The calculated grafting density of the PNIPAAm chain on the AAO surface was  $3.94 \text{ nm}^2$  per chain (eqn (S3) in ESI†). As its radius of gyration is *ca.* 1.0 nm based on a random coil model, the grafted PNIPAAm chains seem to form a

brush-type layer having a thickness of only about 2.0 nm. Based on this model, the hydrodynamic effect was about six times more significant as compared to the effect of pore enlargement. Therefore, instead of the change of the pore size, it is likely that the rapidly increasing diffusivity is induced by the hydrophobicity of the PNIPAAm-grafted surface. On a hydrophobic pore surface, dextran molecules become less hydrogen-bonded, decreasing the interaction with the PNIPAAm coated surface that can enhance the effective partitioning of FITC-dextran into the nanopore.<sup>10</sup> To additionally confirm the effect of hydrophobic coating on dextran diffusion, the diffusivity through the nanopores modified with 4-*tert*-butylcatechol was also examined. The diffusion through PNIPAAm-grafted nanopores was as fast as that through 4-*tert*-butylcatechol modified nanopores at 42 °C ( $2.31 \times 10^{-8} \text{ cm}^2 \text{ s}^{-1}$ ), which obviously demonstrates that the hydrophobic transition of surface wettability in response to the temperature change is responsible for such dramatic increase in the diffusion of FITC-dextran through the PNIPAAm-grafted nanopores.

We have described a facile method to thermally control the surface wettability of nanopores by grafting catechol-tethered PNIPAAm to the surface of alumina. The thermosensitive change of surface wettability was used as a means of controlling the diffusional permeability of a solute through nanopores. This new underlying mechanism of grafting is distinct from the previously reported systems based on the physical pore blocking of entangled polymer chains.<sup>9</sup> Although optimal conditions need to be further explored, it is expected that the simple surface coating for temperature-sensitive grafting of nanoporous materials can be applied to chemical separation or biological sensors.

This study was financially supported by a grant of the Korean Health Technology R&D Project, Ministry of Health and Welfare (A040041 and A111552), Republic of Korea.

## Notes and references

- 1 M. S. Yavuz, Y. Y. Cheng, J. Y. Chen, C. M. Copley, Q. Zhang, M. Rycenga, J. W. Xie, C. Kim, K. H. Song, A. G. Schwartz, L. H. V. Wang and Y. N. Xia, *Nat. Mater.*, 2009, **8**, 935–939.
- 2 (a) M. Hesampour, T. Huuhilo, K. Mäkinen, M. Manttari and M. Nyström, *J. Membr. Sci.*, 2008, **310**, 85–92; (b) M. Yang, L. Y. Chu, H. D. Wang, R. Xie, H. Song and C. H. Niu, *Adv. Funct. Mater.*, 2008, **18**, 652–663.
- 3 B. H. Kim, D. H. Lee, J. Y. Kim, D. O. Shin, H. Y. Jeong, S. Hong, J. M. Yun, C. M. Koo, H. Lee and S. O. Kim, *Adv. Mater.*, 2011, **23**, 5618–5622.
- 4 J. H. Waite and M. L. Tanzer, *Science*, 1981, **212**, 1038–1040.
- 5 (a) K. Kaleem, F. Chertok and S. Erhan, *Nature*, 1987, **325**, 328–329; (b) H. Lee, K. Lee, I. K. Kim and T. G. Park, *Adv. Funct. Mater.*, 2009, **19**, 1884–1890.
- 6 R. Narain, M. Gonzales, A. S. Hoffman, P. S. Stayton and K. M. Krishnan, *Langmuir*, 2007, **23**, 6299–6304.
- 7 (a) C. W. Scales, A. J. Convertine and C. L. McCormick, *Biomacromolecules*, 2006, **7**, 1389–1392; (b) J. W. Chan, B. Yu, C. E. Hoyle and A. B. Lowe, *Polymer*, 2009, **50**, 3158–3168.
- 8 M. S. Toprak, B. J. McKenna, J. H. Waite and G. D. Stucky, *Chem. Mater.*, 2007, **19**, 4263–4269.
- 9 (a) P. F. Li, R. Xie, J. C. Jiang, T. Meng, M. Yang, X. J. Ju, L. H. Yang and L. Y. Chu, *J. Membr. Sci.*, 2009, **337**, 310–317; (b) O. Schepelina and I. Zharov, *Langmuir*, 2007, **23**, 12704–12709.
- 10 L. F. Scatena, M. G. Brown and G. L. Richmond, *Science*, 2001, **292**, 908–912.